The Astrophysical Journal, 616:1301–1310, 2004 December 1

NEW LABORATORY DATA ON A MOLECULAR BAND AT 4429 Å

M. Araki, H. Linnartz,[1] P. Kolek, H. Ding, A. Boguslavskiy, A. Denisov, T. W. Schmidt, T. Motylewski, P. Cias, and J. P. Maier
Department of Chemistry, University of Basel, Klingelbergstrasse 80, CH-4056 Basel, Switzerland; mitsunori.araki@unibas.ch, linnartz@few.vu.nl, p.kolek@unibas.ch, hongbin.ding@unibas.ch, a.boguslav@unibas.ch, alexey.denisov@unibas.ch, t.schmidt@chem.usyd.edu.au, t.motylewski@bfad.de, pawel@stan.chemie.unibas.ch, j.p.maier@unibas.ch
Received 2004 April 13; accepted 2004 July 30

ABSTRACT

New laboratory data are presented for the previously reported molecular absorption band at 4429 Å observed in a benzene plasma matching the strongest diffuse interstellar band (DIB) at 4428.9 Å. Gas-phase absorption spectra are presented for rotational temperatures of ~15 and 200 K. The observations indicate that it is unlikely that the laboratory band and the 4429 Å DIB are related. Eleven isomers of $C_5H_5^{(+)}$ and $C_6H_5^{(+)}$, both neutral and cationic, were considered as possible carriers of the laboratory band in view of the observed rotational profiles and deuterium isotope shifts. The experimental data and theoretical calculations (CASPT3, MRCI) indicate that the HCCHCHCHCH radical, a planar but nonlinear chain with one hydrogen on each carbon, is the most probable candidate causing the 4429 Å laboratory absorption.

Subject headings: ISM: lines and bands — ISM: molecules — line: identification — methods: laboratory — molecular data

1. INTRODUCTION

Recent progress with sensitive optical spectroscopic techniques allows the detection of gas-phase spectra of molecules that have been considered as potential carriers of diffuse interstellar bands (DIBs). The DIBs are observed as absorption features toward reddened stars (Herbig 1975). Up to now over 200 such features have been reported (Jenniskens & Désert 1994; Tuairisg et al. 2000), varying in width and intensity. It is a long-standing problem to explain their origin. Various forms of matter have been proposed, but none have resulted in an unambiguous assignment (Tielens & Snow 1995). The report in this journal (Ball et al. 2000) of a striking match between a laboratory band at 4429 Å measured through an expanding benzene plasma and the strongest DIB, centered at 4428.9(1.4) Å, has attracted attention, initiating a discussion on whether radical fragments of aromatic rings might be present in the diffuse interstellar medium (Thaddeus & McCarthy 2001).

In their thorough spectroscopic study of a hydrocarbon plasma, Ball et al. find a strong molecular band at 4429.27(4) Å consisting of an unresolved *P*-, an unresolved *Q*-, and an unresolved *R*-branch, matching in wavelength to a few parts in 10^4 the 4429 DIB. They conclude from partial and complete deuteration of the precursor gas benzene that the laboratory carrier is a hydrocarbon of the form $C_nH_5^{(+)}$ with two pairs of equivalent hydrogen atoms plus a single hydrogen. They discuss a series of possible radicals and propose as most likely candidates the quasi-linear benzene fragments $C_3H_5^+$ and C_5H_5, for which optical data have not been reported.

While the match in wavelength between the laboratory and astronomical spectra is striking, there is no agreement in their line widths; the 4429 DIB feature is about 17 times wider than the band observed in the jet. In two recent studies of the intrinsic profile of the 4429 DIB (Snow 2002; Snow et al. 2002), the lack of fine structure is attributed to an electronic transition of a gaseous molecule with the upper state undergoing a rapid internal conversion, or alternatively a system consisting of overlapping rotational lines. The first explanation implies that the laboratory and astronomical spectra are identical both in wavelength and in line width, which is not the case. The second explanation leaves space for the proposition by Ball et al. that the mismatch in line width may be due to a substantial difference in rotational temperature of the carrier in a supersonic beam (a few K), where collisional cooling is the main relaxation mechanism, and in interstellar space (a few hundred K), where radiative cooling might be very inefficient for weakly polar species. Hence measuring the same spectrum at different temperatures will give additional information on the astrophysical relevance of the 4429 Å molecular band. Moreover, the discussion will benefit from the identification of the carrier of the laboratory spectrum.

2. EXPERIMENT

The results of two complementary laboratory experiments are described. The first is similar to that reported by Ball et al. (2000); the 4429 Å band has been recorded through a benzene plasma generated in a planar supersonic jet at rotational temperatures of 15–40 K. In the second a hollow cathode discharge cell is used instead, resulting in a substantially higher rotational temperature of about 200 K. In both experiments, cavity ring-down (CRD) spectroscopy is used as a sensitive detection technique to observe signals in direct absorption (O'Keefe & Deacon 1988). Very long absorption path lengths are obtained by confining the light tens of microseconds in the cavity.

In the first experiment a cooled planar plasma is generated by applying a 500 μs voltage pulse (−700 to −900 V) to a 1 ms gas pulse of a 0.3% C_6H_6/Ar (C_6D_6/Ar) mixture that is expanded through a 3 cm × 300 μm slit with a backing pressure of about 10 bars. This setup has been used in the study of over 20 hydrocarbon radicals and cations up to now (see, e.g., Motylewski et al. 2000) and combines high molecular densities with an effective adiabatic cooling. The resolution is increased

[1] Current address: Laser Centre and Department of Physical Chemistry, De Boelelaan 1083, NL-1081 HV, Amsterdam, Netherlands.

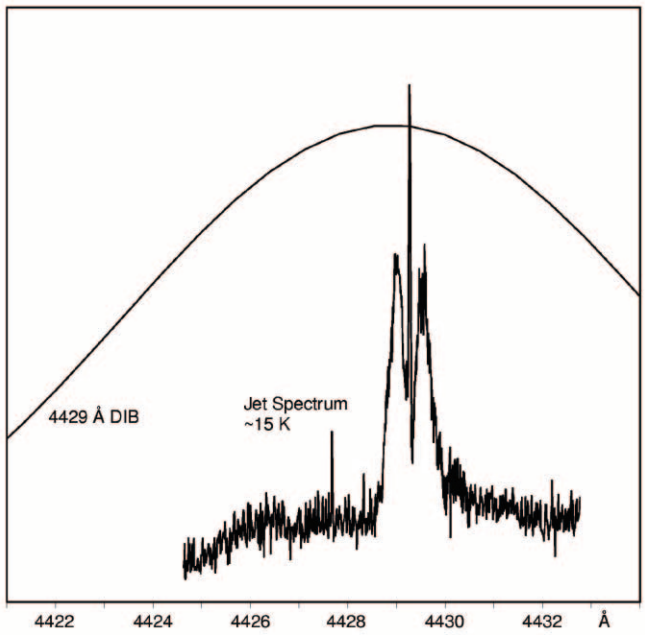

FIG. 1.—The 4429 Å absorption band observed through a planar benzene plasma expansion using a CRD approach. The band coincides in wavelength with the 4429 Å DIB (taken from Jenniskens & Désert 1994 as shown in part above), but the line widths of the laboratory and astronomical spectra differ significantly.

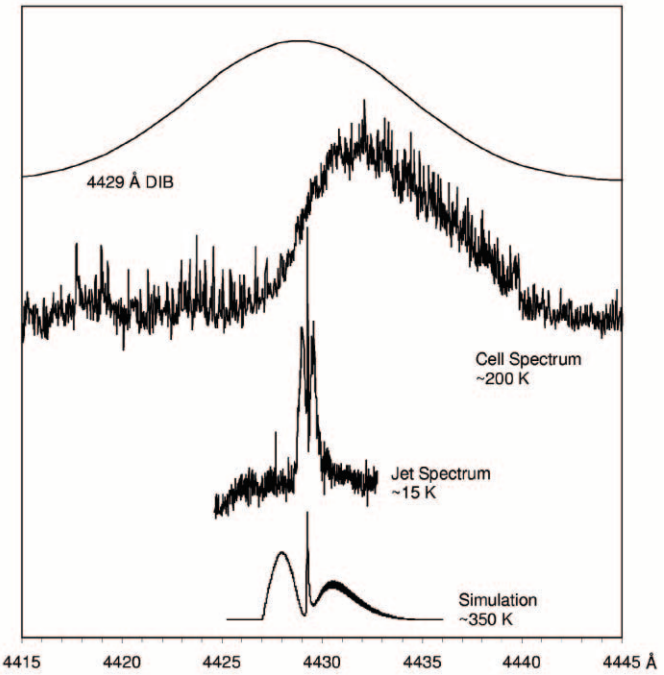

FIG. 2.—The 4429 Å absorption band measured in a jet and liquid nitrogen cooled hollow cathode discharge cell and compared to the 4429 Å DIB (taken from Jenniskens & Désert 1994). At the higher temperature a clear broadening is observed. A simulated rotational profile at 350 K, using the same constants as in Fig. 3, is clearly different from the observed cell spectrum.

compared to pinhole expansions as used by Ball et al. (2000) because of reduced Doppler broadening parallel to the slit that allows spectroscopy at the limit of the laser resolution. Rotational temperatures are slightly higher, typically 15–40 K.

A much warmer plasma is obtained in the second experiment by applying a 500 μs voltage pulse (-1000 V) to gas mixtures identical to those used in the jet, but in an 84 cm long hollow cathode discharge cell, running at a pressure of a few mbar. The spectroscopy is not Doppler-free, and with liquid nitrogen cooling, rotational temperatures are typically 150–200 K (Kotterer et al. 1996).

3. RESULTS AND DISCUSSION

3.1. *Comparison between the* 4429 Å *DIB and Laboratory Bands*

Figure 1 shows the CRD spectrum obtained through the supersonic planar plasma. Although the signal-to-noise ratio is good, no rotational structure is observed that could provide structural information that is necessary to identify the carrier. This indicates either that the separation between adjacent lines is smaller than 0.03 cm^{-1} or that a lifetime broadening exists. The absorption profile is in the middle of the strong 4429 Å DIB as seen from the synthetic spectrum shown in Figure 1. As discussed by Ball et al. (2000), there is a clear difference in spectral width of both features, and this has to be explained before a correlation between the laboratory and astronomical spectra can be established. Ball et al. correctly argue that for the proposed nearly symmetric prolate top molecules, a spectrum consisting of a *P*-, a *Q*-, and an *R*-branch is expected similar to the one observed, under the explicit condition that only the lowest *K* ladder in the ground state is populated. The many subbands from the higher *K* ladders of the ground state may fill out the contour at higher temperatures, causing the observed spectrum to broaden symmetrically, as observed recently for the nonlinear carbon chain $C_6H_4^+$ (Araki et al. 2003). Therefore the same spectrum was recorded under warmer conditions than in the jet expansion. Decreasing the backing pressure, increasing the benzene/mixing ratio, measuring closer to the jet, and using higher discharge voltages generally increases the rotational temperature from 15 to 30–40 K. Indeed, we observed a small shift in the Boltzmann maximum to higher *J*-values, but no broadening could be observed. Consequently, a cell discharge was then used to obtain a much higher temperature.

In Figure 2 the absorption spectrum recorded in a liquid nitrogen cooled hollow cathode cell is shown. The rotational temperature under these conditions is about 200 K. A band broadened asymmetrically to the red is now observed (Fig. 2, with the jet spectrum shown as a reference). Such a broadening is typical for a hot-band progression and quite possible at the high ambient temperatures in the cell. Nevertheless, the spectrum does not fill up the 4429 Å DIB. In order to be sure that the cell and jet spectra are due to the same carrier, the experiment was repeated with fully deuterated benzene as precursor; the absorption feature shifts 123(1) cm^{-1} to higher energy, which is identical to the shift observed in the jet study: 122.8 cm^{-1} (Ball et al. 2000). These observations seem to indicate that the laboratory band and the 4429 Å DIB originate from different carriers.

In order to compare the laboratory and astronomical spectra it would be helpful to know more about the vibrational temperature ($T_{\rm vib}$) in the cell plasma, but without the detection of a resolved transition from a vibrationally excited level in the ground state it is hard to determine this value. Generally, vibrational temperatures in a cooled cell discharge vary from a few hundred to a thousand kelvins according to similar discharge systems (Zelinger et al. 2003; Greenberg & Hargis 1990). The determination of rotational temperatures ($T_{\rm rot}$), e.g., 200 K for N_2^+ (Kotterer et al. 1996) and 500–600 K for D_3O^+ (Araki et al. 1999) put a lower limit to $T_{\rm vib}$. Such values are indeed

sufficiently high to excite low-frequency vibrational modes in molecules the size of C_5H_5. A broadening due to a series of hot-band progressions is therefore reasonable to assume.

On the other hand, in the plasma jet expansion such bands are not expected. It has been shown that these low rotational temperatures at high vibrational temperatures are obtained for small (diatomic) molecules (Bazalgette Courrèges-Lacoste et al. 2001), but for larger species with smaller vibrational spacings, rotational and vibrational temperatures will be more similar. As a consequence, hot-band progressions are not observed. Nevertheless, because the cooling and heating mechanisms in space are completely different from those in the laboratory, care has to be taken when comparing the CRD spectrum with the 4429 Å DIB.

3.2. *Comparison between the* 4429 Å *DIB and the Simulated Spectrum*

We have made a substantial effort to identify the carrier of the laboratory band by combining experimental and theoretical information. The 4429 Å absorption band has been reproduced using the program WANG (Luckhaus & Quack 1989). It is found that an "*a*-type transition" of a nearly prolate top with rotational constants $A \sim 1$ and $B \approx C \sim 0.1$ cm^{-1} reproduces the observed spectrum under the assumption that the molecular geometry change upon electronic excitation is small and that differences of rotational constants in the two electronic states are less than 1%. A simulated spectrum for 15 K is shown in Figure 3. For B and C values larger than 0.1 cm^{-1}, a resolved rotational profile is expected, which is not the observation. As a consequence, molecules with less than five carbon atoms are not considered. Furthermore, the production of molecules with more than six carbon atoms or with a four-membered ring is not favored in the benzene discharge. Additional information is available from the observation of deuterium isotope shifts by Ball et al. (2000) that indicates that the carrier contains five hydrogen atoms, including two pairs of equivalent ones. These considerations result in 11 isomers of $C_5H_5^{(+)}$ and $C_6H_5^{(+)}$ (Fig. 4), both neutral and cationic, as the most probable carriers of the laboratory spectrum. Anions are not considered since their production is not favored under the conditions used in the CRD experiment.

We have simulated the profile with $T_{\rm rot} = 350$ K (Fig. 2). This indicates that our cell spectrum cannot be reproduced by a rotational profile of the origin-band alone. This is consistent with the proposed explanation that the cell spectrum is the result of overlap of such rotational profiles for various vibrational hot-band transitions. Furthermore, the simulation at $T_{\rm rot} = 350$ K indicates the profile of the 4429 Å DIB cannot be reproduced by a rotational profile of the origin-band alone. In the jet spectrum the intensity of the *R*-branch is stronger than that of *P*, because the ground-state rotational constant $(B + C)/2$ is larger than in the excited state. At high temperatures the intensity difference between the *R*- and *P*-branches increases and the rotational profile becomes asymmetric, although the 4429 Å DIB has a symmetric Lorentzian profile (Snow et al. 2002).

As vibrational frequencies in excited electronic states are generally lower than in the ground state, the hot-band transitions are usually to the red of the origin band. This is as seen in the cell spectrum at $T_{\rm vib} = 200$ K, where the profile extends asymmetrically to the red. Thus it does not seem realistic that the profile to the blue of the origin band could be filled by hot-band transitions even at very high values of $T_{\rm vib}$. Our conclusion is that the laboratory band and the 4429 Å DIB are unlikely to originate from the same carrier.

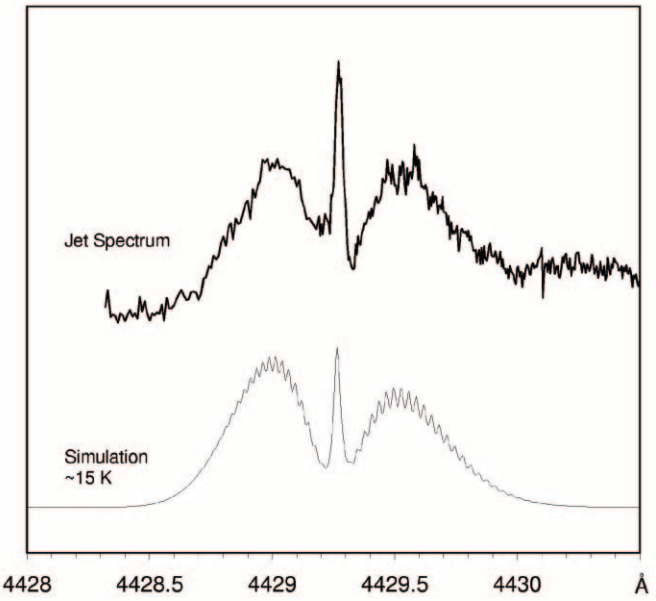

FIG. 3.—Simulated *a*-type rotational profile of the 4429 Å electronic transition for a prolate molecule at 15 K compared to the laboratory absorption spectrum.

3.3. *Identification of the* 4429 Å *Laboratory Band*

Calculations of vertical excitation energies and transition moments were carried out for various C_5H_5 and C_6H_5 species (Fig. 4) using the TD-DFT (B3LYP) method with the Gaussian program (Frisch et al. 2003). For selected molecules, higher accuracy excitation energies (vertical and adiabatic) and rotational constants in the ground and excited states were computed with the CASSCF, CASPT3, and MRCI methods, with the MOLPRO 2002.3 package (Werner & Knowles 2003); see Appendix for the computational details. The cc-pVDZ basis set was used in all calculations.

The electronic transition must fulfill four conditions for the molecule to be regarded as a possible carrier for the laboratory band: (1) it must have excitation energy close to the experimental value of 2.80 eV, (2) it must have a nonzero oscillator strength, (3) the transition dipole moment must be predominantly along the *a*-axis ($|\mu_a| \gg |\mu_b|$ and $|\mu_a| \gg |\mu_c|$), and (4) it must have small differences of rotational constants between the ground and excited states. At the TD-DFT stage of calculations, a vertical excitation energy around 2.8–3.1 eV is required. Conditions 1–3 are fulfilled by the neutral radical $5a^N$ and the cation $5b^+$, but they are not fulfilled by any of the C_6H_5 species, either neutral or cationic (Table 1). The TD-DFT method was found useful because it gives vertical excitation energies with a reasonable accuracy (including dynamical correlation) at relatively low computational cost. However, this method is not applicable for 5*d* and 5*e* because of the complicated electronic structures (§ A2). CASSCF calculations for the 5*d* species [doublet $5d^N(D)$ and quartet $5d^N(Q)$ for neutral and singlet $5d^+(S)$ and triplet $5d^+(T)$ for cation] are presented in the Appendix. Calculated electronic structures and spectroscopic parameters of 5*d* and 5*e* are almost the same.

In order to judge whether the carrier of the 4429 Å band is a neutral or a cation, an additional experiment has been carried out. In this the 4429 Å transition was searched for in a benzene plasma with a resonant two-color two-photon ionization (R2C2PI) approach (Ding et al. 2003), capable of measuring the masses of the neutral radicals selectively. The discharge systems used in the R2C2PI and CRD setups are

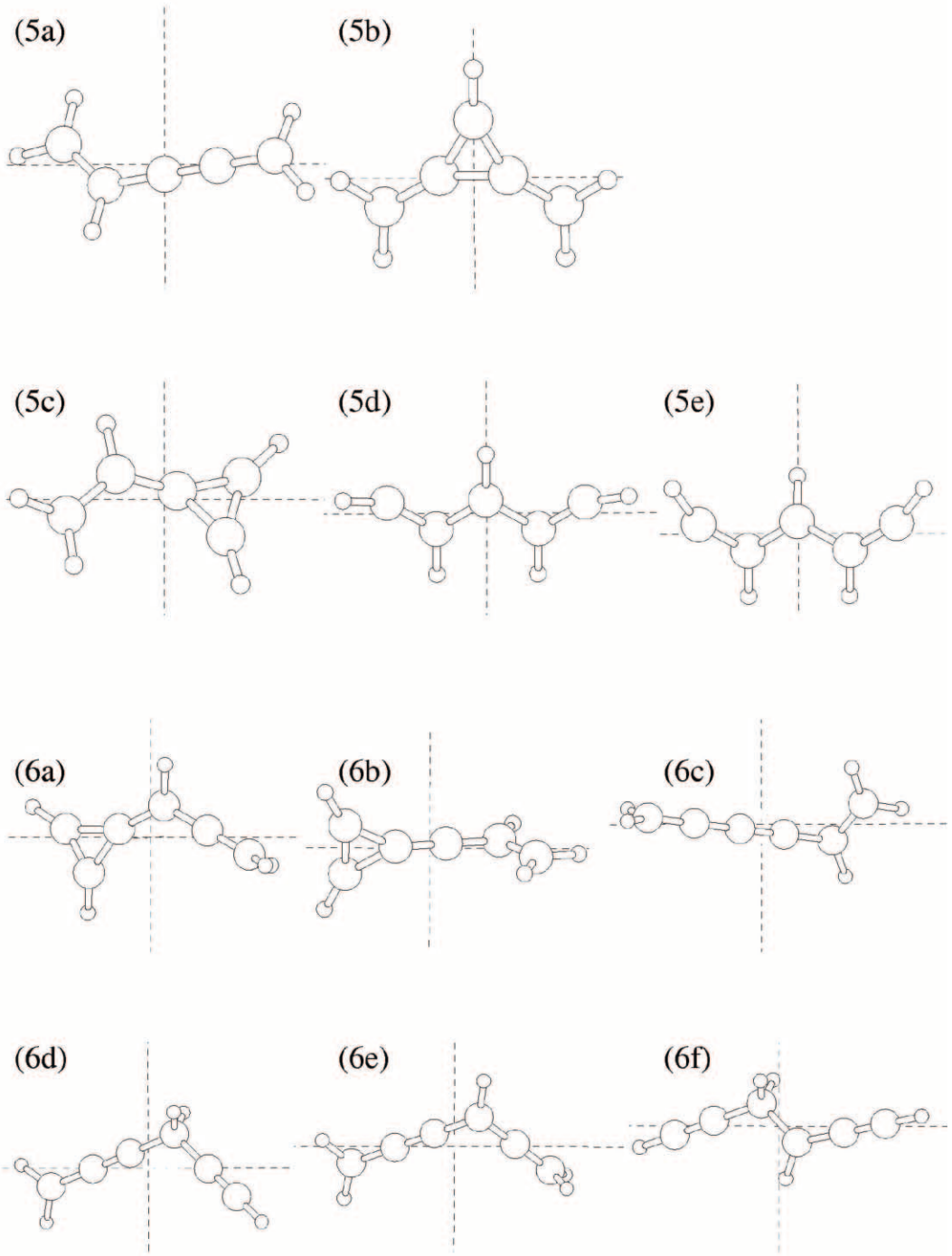

FIG. 4.—Eleven possible C_5H_5 and C_6H_5 isomers with two pairs of equivalent hydrogen atoms and a prolate structure. The horizontal dashed line indicates the *a*-axis, the vertical one the *b*-axis; the *c*-axis is perpendicular to the plane formed by *a* and *b*.

comparable, and experiments have been performed using similar conditions. A 0.4% C_6H_6/Ar mixture (backing pressure 5 bars) was discharged between two stainless steel electrodes mounted in the ceramic body of a pinhole source. The excitation laser was scanned around 4429 Å, and intense radiation from an F_2 laser (157 nm) or Nd : YAG (212.5 nm) was used for the ionization. Neutral species with an ionization potential of less than 10.7 eV are detected in this way. All species with a mass of less than 200 amu have been monitored simultaneously.

A weak band of neutral C_5H_5 was observed at 4435 Å, but no band at 4429 Å could be seen (Fig. 5). This suggests that the carrier of the 4429 Å laboratory band either is a charged species, or a neutral one with an ionization potential higher than 10.7 eV, or has a very short upper electronic state lifetime. It is also possible that the species is destroyed by chemical reactions before reaching the mass spectrometer because in the R2C2PI experiment the molecular beam is probed 30 cm downstream, but only 2 mm downstream in the CRD experiment.

The profiles of the 4429 Å CRD absorption (Fig. 1) and the R2C2PI C_5H_5 band (Fig. 5) are similar, indicating that the molecules probably have similar geometries. The R2C2PI band can be reproduced by a simulation of the rotational profile based

TABLE 1

VERTICAL ELECTRONIC TRANSITIONS OF C_5H_5 AND C_6H_5 CALCULATED USING TD-DFT METHOD

	Neutral					Cation				
			Transition Moment (D)					Transition Moment (D)		
Isomer[a]	ΔE[b] (eV)	f[c]	μ_a	μ_b	μ_c	ΔE[b] (eV)	f[c]	μ_a	μ_b	μ_c
5*a*.....	2.93	0.000	0.000	0.000	0.012	2.36	0.000	0.000	0.000	0.022
	2.98[d]	0.003	−0.514	−0.016	0.000	4.37	0.498	5.475	0.281	0.000
5*b*.....	2.22	0.073	2.948	0.000	0.000	3.09[d]	0.190	−4.032	0.106	0.000
	3.86	0.000	0.000	0.000	−0.065	3.36	0.000	0.000	0.000	−0.105
5*c*.....	1.57	0.002	−0.097	0.576	0.000	5.62	0.102	−1.861	−1.145	0.000
	3.94	0.001	0.065	−0.272	0.000	5.86	0.391	−4.071	−1.019	0.000
6*a*.....	1.35	0.002	0.260	0.557	0.000	4.05	0.000	0.000	0.000	−0.007
	2.72	0.000	0.000	0.000	−0.004	5.35	0.000	0.001	0.000	0.007
6*b*.....	2.34	0.000	0.000	−0.019	0.000	1.89	0.000	0.000	0.027	0.000
	2.93	0.000	−0.008	0.000	−0.069	5.03	0.430	4.692	0.000	−0.729
6*c*.....	2.38	0.000	−0.002	0.000	−0.008	2.05	0.000	0.008	−0.002	−0.014
	2.70	0.000	0.002	−0.001	0.017	4.07	0.245	3.943	−0.568	0.000
6*d*.....	3.15	0.000	0.000	−0.001	0.036	1.39	0.000	0.002	0.001	0.121
	4.16	0.041	−1.547	0.483	0.000	1.72	0.068	3.226	−0.004	−0.001
6*e*.....	3.05	0.000	0.001	0.000	−0.001	2.56	0.000	0.000	0.000	0.005
	3.07	0.001	0.271	−0.184	0.000	2.98	0.000	0.000	0.000	−0.045
6*f*.....	3.35	0.000	0.000	0.000	−0.004	1.40	0.000	0.007	−0.002	−0.124
	4.02	0.028	−1.353	−0.081	0.000	1.73	0.070	3.235	−0.379	0.001

NOTE.—B3LYP hybrid functional and the cc-pVDZ basis set were used.

[a] See Fig. 4.

[b] The observed adiabatic transition energy is 2.80 eV (=4429 Å).

[c] Oscillator strength.

[d] For higher level calculations see Tables 2 and 3.

on the assumptions that the transition is *a*-type and that the carrier is a nearly prolate C_5H_5 molecule at 7 K, a typical temperature of the molecules produced in this apparatus. Simulation at 15 K with the same molecular constants can reproduce the profile of the 4429 Å CRD band. Thus it appears that both the carrier of the 4429 Å CRD and the 4435 Å resonance-enhanced multiphoton ionization (REMPI) band have five carbon atoms, but are different isomers.

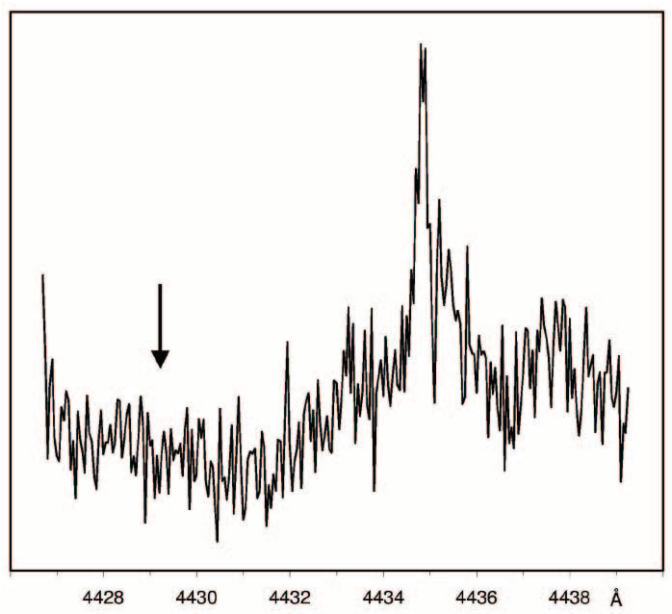

FIG. 5.—Absorption spectrum recorded through a benzene plasma at mass 65 amu (C_5H_5) in the 4429 Å region using a two-laser photon excitation scheme. A 2125 Å laser was used for the ionization step. The 4435 Å band detected has a profile similar to that of the 4429 Å band in the CRD spectrum of Fig. 1. Position of the 4429 Å band in the CRD spectrum is indicated by the arrow.

The 5*e* isomer cannot convert to cyclic pentadienyl radical as easily as 5*d* because additional cis-trans isomerizations are difficult. The isomer does not decay as fast and may be one of the possible candidates for the REMPI band. For the same reason production of 5*d* should be favored and a larger abundance of this isomer could be expected immediately after the discharge through benzene. Therefore 5*d* would be a better candidate for the carrier of the CRD band.

Higher level theoretical calculations were carried out for the $5a^N$, $5b^+$, $5d^N(D)$, $5d^N(Q)$, $5d^+(T)$, $5e^N(D)$, $5e^N(Q)$, and $5e^+(T)$ species with the CASPT3 (Werner 1996; Celani & Werner 2000) and MRCI methods (Werner & Knowles 1988; Knowles & Werner 1988). The $5d^+(S)$ and $5e^+(S)$ isomers were not considered at this stage because the CASSCF results indicate too-high excitation energies of 4.6 eV for the lowest *a*-type transitions (see § A1). The active space, including seven orbitals (five π-orbitals perpendicular to the molecular plane, and two in-plane orbitals), was used with seven electrons for a neutral radical and six for a cation. The vertical and adiabatic transition energies are given in Table 2. The transitions $2\,^2A_2 \leftarrow {}^2B_1$ of $5d^N(D)$ and $^3A_1 \leftarrow {}^3B_2$ of $5d^+(T)$ (both in C_{2v} symmetry) have adiabatic excitation energies of 2.72 and 2.75 eV, respectively, at the CASPT3 level of theory, which are close to the experimental value of 2.80 eV. The same transitions of $5e^N(D)$ are 0.02 eV lower than those of $5d^N(D)$ (CASPT3). This is an additional reason for the assignment of the 4429 Å CRD band. The smallest differences between vertical and adiabatic excitation energies predicted for $5d^N(D)$, $5e^N(D)$, $5d^+(T)$, and $5e^+(T)$ are consistent with the analysis of the rotational profile and may suggest a small geometry change upon electronic excitation. We searched for a transition up to 2400 cm^{-1} to the blue

TABLE 2
ELECTRONIC TRANSITION ENERGY CALCULATED AT THE MRCI AND CASPT3 LEVEL OF THEORY FOR THE A-TYPE TRANSITION

Isomer[a]	Transition	Method	Adiabatic[b] (eV)	Vertical (eV)	(Vertical) − (Adiabatic) (eV)
Observed	...	...	2.80	...	...
$5a^N$	$^2A''$–$^2A''$	CASPT3	2.39	2.64	0.25
	...	MRCI	2.42	2.69	0.27
	...	MRCI+D	2.40	2.66	0.26
$5d^N(D)$	2^2A_2–$^2B_1$	CASPT3	2.72	2.87	0.15
	...	MRCI	2.68	2.84	0.16
	...	MRCI+D	2.65	2.84	0.19
$5d^N(Q)$	$^4B_1$–$^4A_2$	CASPT3	2.62	2.84	0.22
	...	MRCI	2.61	2.83	0.22
	...	MRCI+D	2.62	2.84	0.22
$5d^+(T)$	$^3A_1$–$^3B_2$	CASPT3	2.75	2.93	0.18
	...	MRCI	2.86	3.06	0.20
	...	MRCI+D	2.81	2.98	0.17
$5e^N(D)$	2^2A_2–$^2B_1$	CASPT3	2.70	2.87	0.17
	...	MRCI	2.64	2.81	0.17
	...	MRCI+D	2.62	2.81	0.21
$5e^N(Q)$	$^4B_1$–$^4A_2$	CASPT3	2.63	2.85	0.22
	...	MRCI	2.63	2.85	0.22
	...	MRCI+D	2.63	2.86	0.23
$5e^+(T)$	$^3A_1$–$^3B_2$	CASPT3	2.72	2.89	0.17
	...	MRCI	2.82	2.97	0.15
	...	MRCI+D	2.78	2.95	0.17
$5b^+$	$^1B_2$–$^1A_1$	CASPT3	3.06	3.39	0.33
	...	MRCI	3.20	3.51	0.31
	...	MRCI+D	3.02	3.31	0.29

NOTE.—The geometries are optimized at the CASPT3 level of theory. For computational details see Appendix.
[a] See Fig. 4.
[b] Adiabatic transition energies without zero vibrational level correction.

of the 4429 Å band using the CRD spectrometer. However, no band that would correspond to vibrational excitation in the upper electronic state was observed in this region either by us or in the study of Ball et al. (2000). Thus the origin band dominates the transition, and the geometry change appears to be small.

Rotational constants in the ground and excited states were calculated at the CASPT3 level of theory by numerical geometry optimization and are given in Table 3. The simulation of the rotational profile of the 4429 Å band suggests that the rotational constants change less than 1% between the two states. The calculated differences in the cases of $5d^N(D)$, $5e^N(D)$ and $5d^N(Q)$, $5e^N(Q)$ agree with the simulation within the errors, and the values of ΔA in the cases of $5a^N$, $5b^+$, $5d^+(T)$, and $5e^+(T)$ are too large.

Good agreement with the experimental data of the 4429 Å CRD band is predicted for the $2\,^2A_2 \leftarrow {}^2B_1$ transitions of $5d^N(D)$ and $5e^N(D)$, although it is slightly better for the first one with all considered criteria. From the candidates discussed we conclude that the $5d^N(D)$ isomer, "planar W structure" with five carbons in C_{2v} symmetry (Fig. 4), a doublet radical, is the most likely carrier of the 4429 Å laboratory band.

This work has been supported by the Swiss National Science Foundation (project 200020-100019).

TABLE 3
ROTATIONAL CONSTANTS CALCULATED AT THE CASPT3 LEVEL OF THEORY

Isomer[a]	Transition	A (cm^{-1})	B (cm^{-1})	C (cm^{-1})	ΔA[b] (%)	ΔB[b] (%)	ΔC[b] (%)
$5a^N$	$^2A''$–$^2A''$	1.235	0.0742	0.0700	−16	1	0
$5d^N(D)$	2^2A_2–$^2B_1$	1.381	0.0792	0.0749	−5	−2	−2
$5d^N(Q)$	$^4B_1$–$^4A_2$	1.378	0.0793	0.0750	−4	−3	−3
$5d^+(T)$	$^3A_1$–$^3B_2$	1.201	0.0828	0.0775	11	−4	−5
$5e^N(D)$	2^2A_2–$^2B_1$	1.079	0.0827	0.0768	−4	−2	−2
$5e^N(Q)$	$^4B_1$–$^4A_2$	1.082	0.0827	0.0768	−4	−2	−2
$5e^+(T)$	$^3A_1$–$^3B_2$	0.963	0.0865	0.0794	13	−6	−4
$5b^+$	$^1B_2$–$^1A_1$	0.452	0.1288	0.1003	−21	2	11

NOTE.—For computational details see Appendix. Rotational constants A, B, and C are in the ground state.
[a] See Fig. 4.
[b] Differences of rotational constants between the ground and excited states.

APPENDIX

COMPUTATIONAL RESULTS AND DETAILS

DFT (B3LYP) geometry optimization and frequency calculation were carried out for the ground state of all molecules, and no imaginary vibrational frequencies were obtained for the investigated ground states. Thus time-dependent perturbation treatment (TD-DFT) was used to calculate vertical excitation energies and transition dipole moments to the first and second electronically excited states (Table 1), although the TD-DFT method is not applicable if the ground state is not characterized by a single configuration and/or if there is a significant contribution of double excitations in the excited state configuration. Therefore the $5d^N(D)$, $5d^N(Q)$, $5d^+(S)$, $5d^+(T)$, and relevant $5e$ isomers were considered separately using the CASSCF method (see §§ A1 and A2). All calculations were done with a cc-pVDZ basis set.

In the CASSCF, CASPT3, and MRCI calculations the active space included five π-orbitals perpendicular to the molecular plane and two in-plane orbitals, with seven electrons for neutral radicals and six electrons for cations. In the case of $5a^N$ the two in-plane orbitals are π and π^* orbitals of the C3≡C4 triple bond; for $5b^+$ the two in-plane orbitals are the $\sigma_{\rm HOMO}$ and $\sigma^*_{\rm LUMO}$ orbitals localized on the three-membered ring. The two in-plane orbitals of the $5d$ isomers are symmetric and antisymmetric combination of two carbon lone-pair orbitals of C1 and C5 carbon atoms. The above choice was preceded by the CASSCF calculations with larger active space, since other orbitals are inactive for the states of interest (the corresponding CI coefficients are smaller than 0.05). In the CASPT3 and MRCI calculations the core orbitals were not correlated. For $5b^+$, $5d$, and $5e$, calculations were executed in a C_{2v} symmetry point group.

The results of CASSCF calculations for manifold excited states of $5d^N$ and $5d^+$ are presented in § A1. These allowed us to identify the excited states of the required adiabatic excitation energies and orientations of the transition dipole moments. The electronic configuration of the ground and excited states of interests are discussed in § A2. The electronic structures and spectroscopic parameters of $5d$ and $5e$ are very similar. The total energy of the $5e^N(D)$, $^2B_1$, is 0.02 eV higher than that of $5d^N(D)$, and the two excitation energies differ by not more than ±0.04 eV. Therefore only the data of $5d$ are listed here. The vertical and adiabatic excitation energies (Table 3) were calculated using CASPT3, MRCI, and MRCI with Davidson correction (MRCI+D) methods for geometries optimized numerically using the CASPT3 method.

A1. ELECTRONICALLY EXCITED STATES OF THE 5*D* MOLECULES

The CASSCF calculations of vertical and adiabatic excitation energies (without ZPE correction) were performed for two states from each irreducible representation of the C_{2v} point group, for each form of the $5d$ molecules: $5d^N(D)$, $5d^N(Q)$, $5d^+(S)$, and $5d^+(T)$. That states cover the energy range up to 4–5 eV. The transition of interest should possess an excitation energy close to the experimental value of 2.80 eV, the required b_2 symmetry (a-type transition), and a significant intensity.

The only relevant transition of $5d^N(D)$ is the $2\,^2A_2 \leftarrow {}^2B_1$ excitation at 2.67 eV (Table A1). A significant transition moment is predicted also for the excitations to the $^2A_1$ and 2^2A_1 states (excitation energies 1.29 and 4.16 eV). For the $5d^N(Q)$ isomer only the $^4B_1 \leftarrow X\ ^4A_2$ excitation is at 2.53 eV (Table A2). A noticeable transition moment is predicted also for the excitations to the $^4B_2$ state (3.40 eV). In the case of $5d^+(S)$, all allowed transitions shown in Table A3 possess rather large transition moments, but the excitation energy of the transitions of the required symmetry ($^1B_2 \leftarrow X\ ^1A_1$ and $2\,^1B_2 \leftarrow X\ ^1A_1$) is too high. All allowed transitions for $5d^+(T)$ shown in Table A4 have rather large transition moments, except for $2\,^3A_1 \leftarrow {}^3B_2$. Among them the $^3A_1 \leftarrow {}^3B_2$ transition has the required symmetry and excitation energy of 2.93 eV. Both the $^3A_1$ and $^3B_2$ states are energetically well separated from other triplet states.

A2. ELECTRONIC STRUCTURE OF THE SELECTED MOLECULES

A2.1. *$5a^N$ and $5b^+$ Isomers*

The main configuration of $5a^N$ in the ground state is 22+00 (0.93), where we show the occupations of the five $\pi\ a''$ active orbitals, with the coefficient given in parentheses, and for the excited state the configurations are 2+200 (0.54), 220+0 (0.49), and 2+−+0 (0.32).

TABLE A1
CASSCF Excitation Energies and Transition Moments for the Doublet Radical $5d^N(D)$

State	Excitation Energy		Transition Moment	
	Vertical (eV)	Adiabatic[a] (eV)	Direction	Value (D)
$^2B_1$	...	...	...	...
$^2A_2$	0.64	0.62	*a*	−0.025
$^2B_2$	1.46	1.19	...	Forbidden
$^2A_1$	1.58	1.29	*c*	−0.241
2^2A_2	2.84	2.67	*a*	0.263
2^2B_1	3.44	3.27	*b*	0.046
2^2A_1	4.42	4.16	*c*	−0.625
2^2B_2	4.51	4.21	...	Forbidden

[a] Adiabatic transition energies without ZPE correction.

TABLE A2

CASSCF Excitation Energies and Transition Moments for Quartet Radical $5d^N(Q)$

State	Excitation Energy		Transition Moment	
	Vertical (eV)	Adiabatic[a] (eV)	Direction	Value (D)
$X\,^4A_2$	...	...	...	...
$^4B_1$	2.79	2.53	*a*	−0.218
$^4A_1$	3.76	3.33	...	Forbidden
$^4B_2$	3.88	3.40	*c*	−0.263
2^4A_2	4.43	4.17	*b*	0.017
2^4B_1	5.18	4.71	*a*	−0.049
2^4B_2	6.03	5.49	*c*	−0.102
2^4A_1	6.13	5.55	...	Forbidden

[a] Adiabatic transition energies without ZPE correction.

TABLE A3

CASSCF Excitation Energies and Transition Moments for Singlet Cation $5d^+(S)$

State	Excitation Energy		Transition Moment	
	Vertical (eV)	Adiabatic[a] (eV)	Direction	Value (D)
$X\,^1A_1$	...	...	...	...
$^1B_1$	3.28	2.27	*c*	−0.473
$^1A_2$	3.49	2.73	...	Forbidden
2^1A_1	3.80	3.61	*b*	−0.625
2^1B_1	4.66	4.58	*c*	0.533
$^1B_2$	4.79	4.61	*a*	6.774
2^1A_2	4.83	4.67	...	Forbidden
2^1B_2	5.34	5.25	*a*	0.529

[a] Adiabatic transition energies without ZPE correction.

TABLE A4

CASSCF Excitation Energies and Transition Moments for Triplet Cation $5d^+(T)$

State	Excitation Energy		Transition Moment	
	Vertical (eV)	Adiabatic[a] (eV)	Direction	Value (D)
$^3B_2$	...	...	...	...
2^3B_2	2.55	2.34	*b*	−0.360
$^3B_1$	2.62	1.67	...	Forbidden
$^3A_2$	2.87	2.16	*c*	0.438
$^3A_1$	3.14	2.93	*a*	0.518
2^3B_1	4.18	4.06	...	Forbidden
2^3A_1	4.37	4.16	*a*	0.012
2^3A_2	4.42	4.21	*c*	−0.546

[a] Adiabatic transition energies without ZPE correction.

TABLE A5
TOTAL ENERGY DIFFERENCE FOR THE LOWEST STATES OF 5*d*

METHOD	ΔE[a] (eV)	
	Neutral Radical $^2B_1$–$X\,^4A_2$	Cation $X\,^1A_1$–$^3B_2$
CASSCF[b]	0.26	−0.05
CASPT3[c]	0.22	−0.05
MRCI[c]	0.23	−0.07
MRCI+D[c]	0.21	−0.06

[a] Energies without ZPE correction.
[b] Geometry optimized with the CASSCF method.
[c] Geometry optimized numerically with the CASPT3 method.

In the case of $5b^+$ in the ground state, these are 200 20 (0.88) and the doubly excited configuration 220 00 (0.39), where we show the occupation of the π-orbitals (three b_1 and two a_2 orbitals), and in the excited state the configurations are 2+0 −0 (+0.64) and 2−0 +0 (−0.64).

A2.2. $5d^N$ and $5d^+$ Isomers

The electronic structure of $5d^N$ and $5d^+$ is more complicated because of the presence of two lone-pair orbitals of carbon atoms C1 and C5 occupied by two electrons. The symmetric and antisymmetric combinations of these orbitals are almost degenerate. The energy difference between the triplet $^3B_2$ and singlet $X\,^1A_1$ states of the $5d^+$ cation is small, 0.05–0.07 eV with all methods (Table A5). The energy of the b_2 excitation (*a*-type transition) of the singlet cation $5d^+(S)$ is rather high, about 4.8 eV vertical and 4.6 eV adiabatic at the CASSCF level, and therefore this molecule was excluded from investigation with the CASPT3 and MRCI methods. The quartet $X\,^4A_2$ state is the lowest energy form of the $5d^N$ radical; the energy of the lowest doublet state $^2B_1$ is 0.21–0.26 eV higher with all methods (Table A5).

The ground-state wavefunctions of the high-spin forms, $5d^N(Q)$ and $5d^+(T)$, are dominated by a single electronic configuration: + 2+0 + 20 (0.94), where we show the occupations of the a_1 carbon lone pair, three b_1 π-orbitals, the b_2 carbon lone pair, and two a_2 π-orbitals, for the quartet radical, and + 200 + 20 (0.94) for the triplet cation. In case of the low-spin forms there are two main configurations of the ground-state wavefunction: 2 200 0 20 (+0.71) and 0 200 2 20 (−0.61) for the singlet cation, and 2 2+0 0 20 (0.66) and 0 2+0 2 20 (0.62) for the doublet radical.

The excited states of interests represent essentially π–π* transitions of b_2 symmetry, although the contribution of the promotion of electrons between the carbon lone-pair orbitals a_1 and b_2 is noticeable, except for the $5d^+(T)$ molecule. The wavefunction of the latter molecule in the excited state $^3A_1$ is mainly a combination of four configurations 1 210 1 10 with all possible spin directions with absolute values of coefficients 0.42–0.50.

The excited-state wavefunction for $5d^N(Q)$ consists of two main configurations: + 220 + +0 (0.60) and + 200 + 2+ (0.57), which represent a π–π transition. Two other configurations, 2 2+0 0 ++ (−0.25) and 0 2+2 2 ++ (+0.25) indicate the contribution of the excitation between the carbon lone-pair orbitals.

The first excitation $1\,^2A_2 \leftarrow {}^2B_1$ of the $5d^N(D)$ doublet radical has an energy of only 0.61 eV (adiabatic transition, CASPT3). That excitation is mainly a promotion of one electron between the carbon lone-pair orbitals a_1 and b_2. The $2\,^2A_2 \leftarrow {}^2B_1$ transition

TABLE A6
GEOMETRY AND ROTATIONAL CONSTANTS COMPUTED WITH CASSCF FOR THE 5*d* ISOMER

PARAMETER	$5d^N(D)$		$5d^N(Q)$		$5d^+(T)$	
	$^2B_1$	2^2A_2	$^4A_2$	$^4B_1$	$^3B_2$	$^3A_1$
Bond length (Å)						
C1-C2	1.362	1.420	1.365	1.443	1.353	1.405
C2-C3	1.422	1.418	1.417	1.404	1.413	1.402
C1-H1	1.080	1.079	1.080	1.080	1.081	1.080
C2-H2	1.088	1.086	1.088	1.086	1.085	1.087
C3-H3	1.082	1.083	1.083	1.084	1.084	1.082
Angle (deg)						
C1-C2-C3	124.594	124.175	124.463	123.813	118.811	123.568
C2-C3-C4	122.991	123.462	123.243	124.068	124.156	120.548
H1-C1-C2	132.317	132.263	131.727	130.056	134.829	134.303
H2-C2-C3	117.699	118.644	117.841	119.009	120.314	119.277
H3-C3-C2	118.505	118.269	118.378	117.966	117.922	119.726
Rotational constant (GHz)						
A	41.601	40.175	41.487	39.440	36.686	40.457
B	2.397	2.333	2.403	2.334	2.517	2.406
C	2.266	2.205	2.272	2.203	2.356	2.271

TABLE A7

Geometry and Rotational Constants Computed with CASPT3 for the 5*d* Isomer

Parameter	$5d^N(D)$		$5d^N(Q)$		$5d^+(T)$	
	$^2B_1$	2^2A_2	$^4A_2$	$^4B_1$	$^3B_2$	$^3A_1$
Bond length (Å)						
C1-C2	1.365	1.442	1.368	1.443	1.364	1.413
C2-C3	1.429	1.408	1.425	1.411	1.422	1.417
C1-H1	1.092	1.090	1.092	1.092	1.096	1.095
C2-H2	1.104	1.096	1.103	1.099	1.100	1.103
C3-H3	1.094	1.089	1.095	1.095	1.098	1.094
Angle (deg)						
C1-C2-C3	124.972	123.803	124.853	124.262	118.802	123.766
C2-C3-C4	122.567	122.887	122.884	123.960	123.754	119.731
H1-C1-C2	134.705	134.863	134.210	132.500	137.062	135.728
H2-C2-C3	117.307	119.027	117.484	118.577	120.464	119.073
H3-C3-C2	118.717	118.556	118.558	118.020	118.123	120.134
Rotational constant (GHz)						
A	41.406	39.410	41.304	39.489	36.015	39.873
B	2.374	2.327	2.377	2.310	2.482	2.365
C	2.245	2.197	2.248	2.182	2.322	2.233

has an excitation energy of 2.72 eV (adiabatic transition, CASPT3), which is close to the experimental value of 2.80 eV and is a promotion of an electron within the π-system from two main configurations of the ground state. The wavefunction of the excited state 2^2A_2 is primarily a combination of four configurations: 2 220 0 +0, 0 220 2 +0, 2 200 0 2+, and 0 200 2 2+, with absolute values of coefficients 0.34–0.39.

A3. EQUILIBRIUM GEOMETRIES OF $5d^N(D)$, $5d^N(Q)$, AND $5d^+(T)$

The geometry parameters and rotational constants were optimized with the CASSCF and CASPT3 methods (Tables A6 and A7, respectively) in C_{2v} symmetry. The vibrational frequencies of the initial states (the lowest state for each multiplicity) were calculated numerically with the CASSCF methods in reduced C_1 symmetry. No imaginary frequencies are present. Efforts were made to calculate the vibrational frequencies of the excited states, but these were not successful because of numerical and convergency problems. Nevertheless, the geometry optimization of the excited states within C_{2v} symmetry seems to be justified, since the excited states of interest are energetically well separated from the neighbor states (Tables A1–A4).

REFERENCES

Araki, M., Linnartz, H., Cias, P., Denisov, A., Fulara, J., Batalov, A., Shnitko, I., & Maier, J. P. 2003, J. Chem. Phys., 118, 10561

Araki, M., Ozeki, H., & Saito, S. 1999, Mol. Phys., 97, 177

Ball, C. D., McCarthy, M. C., & Thaddeus, P. 2000, ApJ, 529, L61

Bazalgette Courrèges-Lacoste, G., Sprengers, J. P., Bulthuis, J., Stolte, S., Motylewski, T., & Linnartz, H. 2001, Chem. Phys. Lett., 335, 209

Celani, P., & Werner, H.-J. 2000, J. Chem. Phys., 112, 5546

Ding, H., Schmidt, T. W., Pino, T., Boguslavskiy, A. E., Güthe, F., & Maier, J. P. 2003, J. Chem. Phys., 119, 814

Frisch, M. J., et al. 2003, Gaussian 03 (rev. A.1; Pittsburgh: Gaussian, Inc.)

Greenberg, K. E., & Hargis, P. J., Jr. 1990, J. Appl. Phys., 68, 505

Herbig, G. H. 1975, ApJ, 196, 129

Jenniskens, P., & Désert, F.-X. 1994, A&AS, 106, 39

Knowles, P. J., & Werner, H.-J. 1988, Chem. Phys. Lett., 145, 514

Kotterer, M., Conceicao, J., & Maier, J. P. 1996, Chem. Phys. Lett., 259, 233

Luckhaus, D., & Quack, M. 1989, Mol. Phys., 63, 745

Motylewski, T., et al. 2000, ApJ, 531, 312

O'Keefe, A., & Deacon, D. A. G. 1988, Rev. Sci. Instrum., 59, 2544

Snow, T. P. 2002, ApJ, 567, 407

Snow, T. P., Zukowski, D., & Massey, P. 2002, ApJ, 578, 877

Thaddeus, P., & McCarthy, M. C. 2001, Spectrochim. Acta A, 57, 757

Tielens, A. G. G. M., & Snow, T. P., eds. 1995, The Diffuse Interstellar Bands (Dordrecht: Kluwer)

Tuairisg, S. Ó., Cami, J., Foing, B. H., Sonnentrucker, P., & Ehrenfreund, P. 2000, A&AS, 142, 225

Werner, H.-J. 1996, Mol. Phys., 89, 645

Werner, H.-J., & Knowles, P. J. 1988, J. Chem. Phys., 89, 5803

———. 2003, MOLPRO (Birmingham: Univ. Birmingham)

Zelinger, Z., Amano, T., Ahrens, V., Brünken, S., Lewen, F., Müller, H. S. P., & Winnewisser, G. 2003, J. Mol. Spectrosc., 220, 223